Reserve Requirements for Wind Power Integration: A Scenario-Based Stochastic Programming Framework

Anthony Papavasiliou, *Student Member, IEEE*, Shmuel S. Oren, *Fellow, IEEE*, and Richard P. O'Neill

Abstract—We present a two-stage stochastic programming model for committing reserves in systems with large amounts of wind power. We describe wind power generation in terms of a representative set of appropriately weighted scenarios, and we present a dual decomposition algorithm for solving the resulting stochastic program. We test our scenario generation methodology on a model of California consisting of 122 generators, and we show that the stochastic programming unit commitment policy outperforms common reserve rules.

Index Terms—Reserve requirements, stochastic unit commitment, wind power integration.

I. INTRODUCTION

THE large-scale integration of wind generation in power systems presents a significant challenge to system operators due to the unpredictable and highly variable pattern of wind power generation. Uncertainty in power system operations is commonly classified in discrete and continuous disturbances. Discrete disturbances include generation and transmission line outages and require the commitment of contingency reserves. Contingency reserves include spinning reserve, online generators which can respond within a few seconds, and nonspinning, or replacement, reserve, which consists of offline generators that replace spinning reserve a few minutes after the occurrence of a contingency in order to restore the ability of the system to withstand a new contingency. Continuous disturbances most commonly result from stochastic fluctuations in electricity demand. The resulting imbalances require the utilization of operating reserves which, as in the case of contingency reserves, are classified according to their response speed. Regulation reserves are capable of responding within seconds in order to maintain system frequency, and load following reserves are re-dispatched in the intra-hour time frame in order to balance larger scale disturbances that occur within the hour.

The unpredictable fluctuations of wind power supply are more naturally categorized as smooth disturbances. Nevertheless, the integration of wind power at a large scale can create significant power shortages that can result in reliability events, such as the 1700-MW wind generation ramp-down that occurred within three and a half hours in Texas in February 2008, and necessitated the curtailment of large industrial customers. Reserve commitment rules have traditionally differentiated between operating and contingency reserves, and have worked effectively in practice for standard system operations. However, the large-scale integration of wind power supply obscures the differentiation between operating reserves and contingency reserves and necessitates more sophisticated methods for dispatching and operating reserves.

Stochastic programming lends itself naturally to the task of optimizing reserve operations due to the fact that reserve dispatch decisions are optimized endogenously in a stochastic programming formulation. In addition to co-optimizing generation schedules and reserve requirements, a stochastic programming model can also be utilized for analyzing the economic impacts of wind integration and demand response in power system operations. Therefore, it is an extremely useful tool both for the purpose of improving system operations but also for analyzing the economic impacts of large-scale renewable power integration.

Despite its attractive features, the application of stochastic programming presents two significant challenges. The first is to develop a methodical approach for selecting and appropriately weighing the scenarios that are input to a stochastic programming formulation. The second challenge is to overcome the computational intractability of the resulting problem. In this paper, we present a methodology for selecting scenarios in stochastic unit commitment problems with large amounts of wind power, and a decomposition algorithm for solving the stochastic program. We validate our scenario selection methodology by comparing the resulting unit commitment policy with standard unit commitment approaches.

II. LITERATURE REVIEW

Our work is motivated by the concerns that were raised in the California ISO 2007 wind integration report [1]. In that report, the California ISO estimates that the target of California to reach a renewable integration level of 20% can increase load following capacity requirements up to 3470 MW, and ramping-up and ramping-down requirements by up to 40 MW/min for up to 20 min, compared to their current levels. Similarly, in a 2006 British report published by the UK Energy Research Center [2], over 80% of the studies that were cited concluded that for wind power integration levels above 20%, an investment in system backup in the range of 5%–10% of installed wind capacity is required in order to balance the short-term (seconds to tens of

A. Papavasiliou and S. S. Oren are with the Department of Industrial Engineering and Operations Research, University of California, Berkeley, Berkeley, CA 94720 USA (e-mail: tonypap@berkeley.edu; oren@ieor.berkeley.edu).

R. P. O'Neill is with the Federal Energy Regulatory Commission, Washington, DC 20037 USA (e-mail: richard.oneill@ferc.gov).

minutes) variability of wind power supply. A 2006 study conducted by Enernex for wind power integration in Minnesota [3] concludes that the cost of additional reserves and costs related to variability and day-ahead forecast errors will increase the cost of wind power production by 2.11 $/MWh (15% penetration) to 4.41 $/MWh (25% penetration).

Unit commitment models are essential for studying the impact of wind power integration in power system operations, due to the fact that operational costs are accurately modeled in a multistage framework. Sioshansi [4] uses a deterministic unit commitment model to perform an annual simulation of wind integration in the ERCOT system, and accounts for load flexibility and transmission constraints. As we described above, the additional advantage of stochastic unit commitment models is the endogenous optimization of reserve commitment. Consequently, stochastic programming has been increasingly utilized in wind integration studies [5]–[8]. Our stochastic programming unit commitment model follows the work of Ruiz *et al.* [9] in formulating a two-stage stochastic program, where the first stage of the problem represents day-ahead unit commitment of slow generators, and the second stage represents hour-ahead economic dispatch of the entire system, given the fixed day-ahead schedule of slow generators. Another appealing feature of the model in [9] which we adopt in our paper is testing unit commitment policies against Monte Carlo samples of wind generation outcomes, instead of the scenario set, since the scenario set holds limited information regarding the behavior of the wind generation resource. Ruiz *et al.* [5] use the general model that they develop in [9] to estimate the impact of wind power integration in the system of the Public Service of Colorado. For the purpose of their annual simulations, Sioshansi [4] and Ruiz [5] solve the unit commitment problem for each day of the year. Although this approach provides a complete picture of annual operations, it is reasonable to expect that much of the information of the model can be captured by focusing the analysis on a representative set of days, thereby reducing computational burden substantially. In particular, we select a representative weekday and weekend for each season, thereby focusing our analysis on eight distinct day types. In addition, we use a decomposition algorithm for solving the stochastic program. In contrast, the authors in [9] solve the stochastic unit commitment problem exhaustively as a mixed integer program. In order to cope with the resulting computational complexity, the authors use a limited number of scenarios and continuous variables for the commitment of fast generators [10], [5].

Bouffard *et al.* [11] introduce a two-stage stochastic programming formulation for modeling reserves that utilizes explicit decision variables for reserves, assuming that reserve bids as well as energy bids are available to the system operator. Bouffard and Galiana [7] use the model developed in [11] to analyze the impact of wind integration on reserve requirements in a small-scale model with three generators and a 4-h horizon without transmission constraints. Morales *et al.* [8] utilize a similar formulation to [7] in order to analyze reserve requirements in the presence of wind power. By aggregating generator unit commitment variables and utilizing a scenario reduction technique, they are able to solve the IEEE 1996 reliability test system with transmission constraints. In contrast to [8], [7], and [11], we focus on a central

unit commitment problem where the ISO strives to minimize operating costs. Therefore, we do not consider reserve bids in our model, since these bids are not associated with an intrinsic cost for generators and should therefore not affect the ISO decision for dispatching resources.

As we mentioned in the introduction, stochastic unit commitment models present computational challenges due to their large scale. A common approach to deal with these challenges is the utilization of decomposition techniques. Such decomposition techniques are used by Takriti *et al.* [12], who use the progressive hedging algorithm of Rockafellar and Wets [13] in order to decompose the stochastic unit commitment problem to single scenario subproblems. Carpentier *et al.* [14] employ an augmented Lagrangian algorithm for solving a multistage stochastic unit commitment problem. Shiina and Birge [15] also employ decomposition by devising a column generation algorithm in order to decompose a multistage stochastic unit commitment problem to single generator subproblems. A heuristic decomposition approach was recently proposed by Zhang *et al.* [16]. In this paper, we employ a Lagrangian relaxation algorithm, in which a first-stage subproblem schedules slow generators and, given these schedules, a set of second-stage subproblems are solved for committing fast generators and dispatching all resources. As we describe in Section B of the Appendix, the advantage of the proposed decomposition is that it allocates computational load evenly among subproblems and yields a feasible solution and upper bound at every step. In addition, it is possible to parallelize the algorithm by solving each second-stage subproblem in a separate processor.

The other major challenge of stochastic unit commitment models is the selection of scenarios and their associated probabilities. Kuska *et al.* [17] present stability results on stochastic programs which motivate an algorithm for scenario selection that strives to minimize the information that is lost by the scenario selection process. Dupacova *et al.* [18] test the algorithm in the context of unit commitment models with load uncertainty. Heitsch and Römisch [19] present faster variants of the algorithm. Morales *et al.* [20] develop an alternative algorithm which resembles the one in [19], but uses a different metric for measuring distances between probability measures. Although there is sound theoretical justification for the algorithm proposed in [19], it suffers from two practical drawbacks for the purposes of our analysis: the algorithm is not consistent with the moments of the wind time series, and the modeler cannot explicitly specify scenarios that are believed to significantly influence the performance of the unit commitment schedule. In this paper, we propose an alternative scenario selection method which addresses these drawbacks.

We test our scenario selection methodology against deterministic reserve rules in a model of the California ISO system consisting of 122 generators and imports from the Western Electricity Coordinating Council (WECC) [21]. We focus our comparison on two types of deterministic reserve rules. The first rule commits reserves by requiring that total reserve in the system is at least a certain fraction of forecast peak load, where the proportionality factor is chosen optimally within a range of reasonable values. The second rule that we test is inspired by a recent report published by the National Renewable Energy Laboratory

[22]. The authors propose a heuristic approach for committing spinning reserves, the 3+5 rule, which requires the system to carry hourly spinning reserve no less than 3% of hourly forecast load plus 5% of hourly forecast wind power. This rule is adapted in our model and we present the results of our comparison in Section V.

III. MODEL

A. Unit Commitment

The stochastic unit commitment model is described by the following minimization problem. Section A of the Appendix describes the nomenclature used in the formulation of the problem.

$$\min \sum_{g \in G} \sum_{s \in S} \sum_{t \in T} \pi_s (K_g u_{gst} + S_g v_{gst} + C_g p_{gst}) \tag{1}$$

s.t.

$$\sum_{g \in G} p_{gst} = D_{st}, t \in T, s \in S \tag{2}$$

$$p_{gst} \leq P_g^+ u_{gst}, g \in G, s \in S, t \in T \tag{3}$$

$$P_g^- u_{gst} \leq p_{gst}, g \in G, s \in S, t \in T \tag{4}$$

$$p_{gst} - p_{gs,t-1} \leq R_g^+, g \in G, s \in S, t \in T \tag{5}$$

$$p_{gs,t-1} - p_{gst} \leq R_g^-, g \in G, s \in S, t \in T \tag{6}$$

$$\sum_{q=t-UT_g+1}^{t} z_{gq} \leq w_{gt}, g \in G_s, t \geq UT_g \tag{7}$$

$$\sum_{q=t+1}^{t+DT_g} z_{gq} \leq 1 - w_{gt}, g \in G_s, t \leq N - DT_g \tag{8}$$

$$\sum_{q=t-UT_g+1}^{t} v_{gsq} \leq u_{gst}, g \in G_f, s \in S, t \geq UT_g \tag{9}$$

$$\sum_{q=t+1}^{t+DT_g} v_{gsq} \leq 1 - u_{gst}, g \in G_f, s \in S, t \leq N - DT_g \tag{10}$$

$$z_{gt} \leq 1, g \in G_s, t \in T \tag{11}$$

$$v_{gst} \leq 1, g \in G, s \in S, t \in T \tag{12}$$

$$z_{gt} \geq w_{gt} - w_{g,t-1}, g \in G_s, t \in T \tag{13}$$

$$v_{gst} \geq u_{gst} - u_{gs,t-1}, g \in G_f, s \in S, t \in T \tag{14}$$

$$\pi_s u_{gst} = \pi_s w_{gt}, g \in G_s, s \in S, t \in T \tag{15}$$

$$\pi_s v_{gst} = \pi_s z_{gt}, g \in G_s, s \in S, t \in T \tag{16}$$

$$p_{gst}, v_{gst} \geq 0, u_{gst}, \in \{0, 1\}, g \in G, s \in S, t \in T \tag{17}$$

$$z_{gt} \geq 0, w_{gt} \in \{0, 1\}, g \in G_s, t \in T. \tag{18}$$

The objective in (1) minimizes startup, minimum load, and fuel costs. As we described in Section II, the stochastic model is a two-stage problem. The first stage of the model represents a day-ahead unit commitment, where the schedules of slow generators are specified. The decisions that are made in this stage cannot be altered once the uncertainty in the system is manifested. The second stage of the model corresponds to hour-ahead operations, and decisions can be adjusted according to the scenario that is realized. In the second stage, we decide about the commitment schedule of fast generators, and the production

plans of all generators. The objective of the stochastic model is to minimize the expected sum of day-ahead commitment costs and hour-ahead commitment and dispatch costs. We also assume the existence of a dummy load with a very high marginal value and no operational constraints, which corresponds to load shedding.

The market clearing constraint in (2) requires that supply matches net demand. Net demand is indexed by scenario because it is uncertain, due to the uncertainty of wind generation. The constraints of (3) and (4) specify the minimum and maximum operating capacity limits of each generator. Equations (5) and (6) model the ramping constraints of each generator. Minimum up and down times are modeled in (7)–(10), following [23]. Note that the integrality of the startup variables v_{gst} can be relaxed in order to reduce the size of the resulting branch and bound tree, which reduces computation time. Equations (11) and (12) are necessary for relaxing the integrality of the startup variables. Equations (13) and (14) model the state transition of the startup variables. The nonanticipativity constraints on the commitment and startup variables are given in (15) and (16).

The deterministic unit commitment problem generates a unit commitment policy that serves as a benchmark for comparing the performance of the stochastic model. The formulation follows [4]:

$$\min \sum_{g \in G} \sum_{t \in T} (K_g w_{gt} + S_g z_{gt} + C_g p_{gt}) \tag{19}$$

s.t.

$$\sum_{g \in G} p_{gt} = D_t, t \in T \tag{20}$$

$$p_{gt} + s_{gt} \leq P_g^+ w_{gt}, g \in G, t \in T \tag{21}$$

$$p_{gt} + s_{gt} + f_{gt} \leq P_g^+, g \in G, t \in T \tag{22}$$

$$p_{gt} \geq P_g^- w_{gt}, g \in G, t \in T \tag{23}$$

$$p_{gt} - p_{g,t-1} + s_{gt} \leq R_g^+, g \in G, t \in T \tag{24}$$

$$p_{g,t-1} - p_{gt} \leq R_g^-, g \in G, t \in T \tag{25}$$

$$\sum_{g \in G} (s_{gt} + f_{gt}) \geq T_{\text{req}}, t \in T \tag{26}$$

$$\sum_{g \in G_f} f_{gt} \geq F_{\text{req}}, t \in T \tag{27}$$

$$(7), (8), (11), (13)$$

$$p_{gt}, z_{gt}, s_{gt}, f_{gt} \geq 0, w_{gt}, \in \{0, 1\}, g \in G, t \in T. \tag{28}$$

Equations (21) and (22) are modified maximum capacity constraints which account for the possibility of generators providing reserves. As in [4], we assume that reserve offers reduce the available generation capacity for energy. Equations (26) corresponds to a total reserve requirement, and (27) corresponds to a fast reserve requirement. There is a day-ahead wind generation forecast which determines forecast net demand. In order to isolate the impact of wind power on operating reserve requirements, we do not model contingency reserves.

B. Economic Dispatch

After the commitment schedule of the slow generators has been determined from the solution of the unit commitment models presented above, the economic dispatch problem is
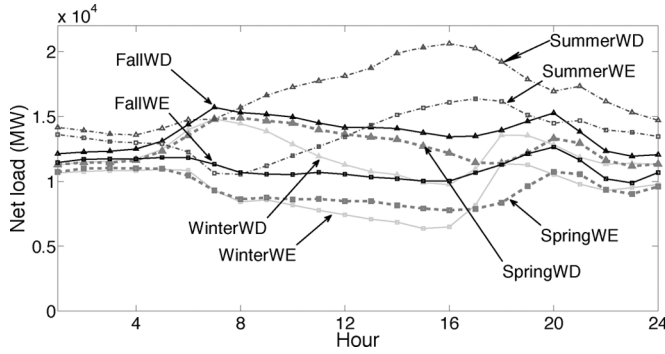
Fig. 1.   Net load for each type of day.

Fig. 2.   Total wind power production versus average wind speed (14% wind).

Fig. 3.   Probability distribution function of average wind speed (14% wind).

solved. The economic dispatch model is derived from the model presented in (19)–(28), with the following exceptions: there are no reserve requirements; the commitment variables of the slow generators are fixed to the values that were determined from the solution of the unit commitment problem; the model is run against samples of wind power generation which are generated according to the wind power model that we describe in the next section; finally, the set of generators G is reduced to the set of generators that were either producing or committed for reserve in the unit commitment model.

As we mentioned in Section II, in contrast to [4] and [5], we focus on eight representative types of days, instead of solving the unit commitment problem for all days of the year. Thus, we are able to avoid resorting to heuristics [10] in order to reduce the computational burden of the analysis, while extracting most of the relevant information from the model. We specify a different type of day for each season, and also differentiate between weekdays and weekends. Hence, the eight types of days include winter weekdays, winter weekends, spring weekdays, and so forth. Each type of day is identified by its forecast net load profile (excluding wind). We note that we have not modeled load forecast uncertainty in our model. The net load profile for each type of day is shown in Fig. 1. For each type of day, we solve the unit commitment problem, which yields a corresponding commitment schedule for slow generators. The Monte Carlo simulations of economic dispatch are then performed, under the presumption that the type of day, therefore the net load excluding wind, is known in advance. For each type of day, we perform economic dispatch for 250 outcomes of wind generation in order to obtain an accurate estimate of the expected performance of each unit commitment policy.

C. Wind Generation

A major difficulty with modeling wind power production is that the mapping of wind speed to wind power production is highly nonlinear. In order to overcome this difficulty, we model wind speed instead of wind power. Given a wind speed model, we follow the approach of Brown *et al.* [24] and Torres *et al.* [25] of using the power curve to model wind power output. However, due to the fact that we are modeling wind production for the entire state, we cannot use the power curve of a single wind generator. Instead, we estimate the aggregate power curve of the entire state by fitting a piecewise linear approximation of average wind speed in the entire state to total power production.
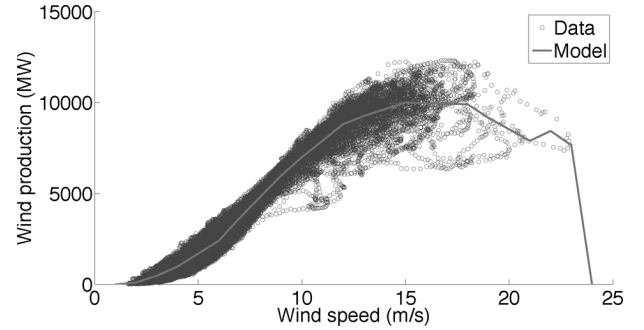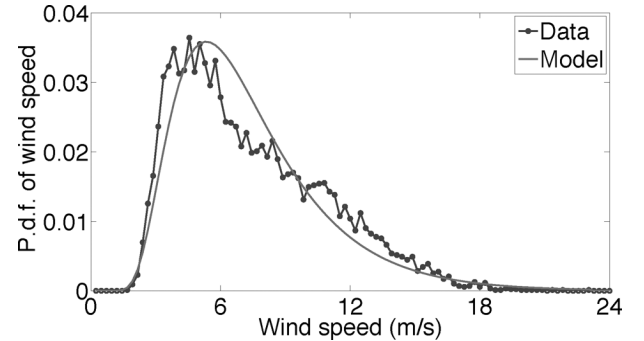
The estimated power curve is superimposed on the data sample in Fig. 2 for one of the two wind integration levels that we are considering in our study. The power curve resembles that of a typical wind generator, although it is smoother due to the geographical diversity of wind generator sites.

As we describe in detail in Section V-A, we model two cases of wind integration, a moderate integration level of 6688 MW and a deep integration level of 14 143 MW. In order to fit the wind speed data, we experimented with various parametric distributions that are suggested in [24], and found the inverse Gaussian distribution to provide the best fit to the wind speed data. The fit is shown in Fig. 3. Once we determine a fit to the wind speed data, we can transform wind speeds to obtain a Gaussian distribution for the transformed data-set:

$$v'_t = N^{-1}(F_{IG}(v_t)) \qquad (29)$$

where $N^{-1}(\cdot)$ is the inverse of the cumulative distribution function of the normal distribution and F_{IG} is the cumulative function of the inverse Gaussian distribution. This is analogous to the wind speed data transformation in [24, (1)], [25, Section 2.1], and [26, (2)] for transforming Weibull-distributed data to Gaussian data, as well as the nonparametric transformation that is used in [27, (8) and (9)].

In order to remove diurnal and seasonal effects, we follow the methodology that is suggested in [24], [25], and [27]. In particular, we calculate the sample mean and variance of transformed wind speeds for each hour of each month, and normalize our data by subtracting the hourly mean and dividing by the hourly standard deviation:

$$v''_t = \frac{v'_t - \mu_{mt}}{\sigma_{mt}} \qquad (30)$$
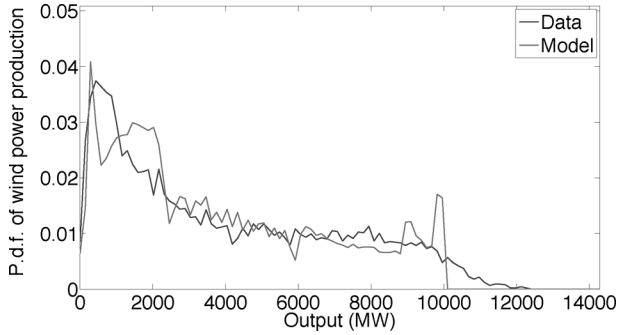
Fig. 4. Probability distribution function of wind power production (14% wind).

where μ_{mt} and σ_{mt} are the mean and standard deviation of v_t' for hour t of month m. The resulting data-set v_t'' is modeled by a third order autoregressive model:

$$v_{t+1}'' = \sum_{k=0}^{2} \phi_k v_{t-k}'' + \sigma\omega \qquad (31)$$

where ω is a standard normal random variable, ϕ_i, $i \in \{1, 2, 3\}$, are the coefficients of the autoregressive model and σ is the variance of the underlying noise. The coefficients of the third order autoregressive model and the variance of the underlying noise are obtained by solving the Yule-Walker equations [28]. Different parameters of the autoregressive model are calculated for the two different cases of wind integration that we study, as we describe in Section V-A.

Once we obtain a third order autoregressive model for the residual of the transformed wind data series, we can work in the opposite direction to simulate wind speed and wind power supply. We use a random number generator to generate residuals through (31), add back diurnal and seasonal effects by inverting (30), and transform the resulting process to wind speed by inverting (29). The resulting process is approximately distributed according to the inverse Gaussian distribution. The fit of our wind speed model to wind speed data for the 14% wind integration case that we study in the results section is shown in Fig. 3. Wind power production is then simulated by using the power curve in Fig. 2. The fit of our model to the data-set for the 14% wind integration case is shown in Fig. 4. The deviations in the fit arise from the fact that the wind speed distribution is not exactly inverse Gaussian and also due to the fact that the power curve cannot exactly reproduce the behavior of the scatter plot in Fig. 2, which is produced by aggregating data from hundreds of locations. Once we have constructed a wind power production model, it is used both for generating wind scenarios, as we will describe next, but also for generating samples for the Monte Carlo simulation of economic dispatch.

IV. SCENARIO GENERATION

The challenge of selecting scenarios for the stochastic unit commitment problem is to discover a small number of representative daily wind time series that properly guide the stochastic program to produce a unit commitment schedule that improves average costs, as compared to a unit commitment schedule determined by solving a deterministic unit commitment model.

The basic tradeoff that needs to be balanced in dispatching fast reserves is the flexibility that fast units offer in utilizing wind generation versus their higher operating costs. Fast generators are fueled by gas, which has a relatively high marginal cost. In addition, the startup and minimum load costs of these units are similar to those of slow units; however, their capacity is smaller. Hence, their startup and minimum load cost per unit of capacity is greater than that of slow generators. The advantage of largely relying on fast units is that the system is capable of discarding less wind power, which results in significant savings in fuel costs. Unlike fast generators which can shut down in short notice in the case of increased wind power generation, slow generators cannot back down from their minimum generation levels and therefore require the waste of excess wind energy in order to stay online.

As we describe in Section II, despite the theoretical justification of the scenario reduction algorithms proposed in [17] and [19], the algorithms are not guaranteed to preserve the moments of hourly wind generation. Due to the predominant role of fuel costs in the operation of the system, the accurate representation of average wind supply in the case of large-scale wind integration is crucial for properly guiding the weighing of scenarios. Moreover, the modeler cannot specify certain scenarios which are deemed crucial. For example, in the case of wind integration, the realization of minimum possible wind output throughout the entire day needs to be considered explicitly as a scenario. Otherwise, there is the possibility of under-committing resources and accruing overwhelming costs from load shedding in economic dispatch. Therefore, it is desirable to develop a scenario selection method which allows us to include such a scenario in the scenario set.

In order to overcome the drawbacks that arise from implementing the algorithms proposed in [17] and [19], we adopt an alternative approach. We generate a large number of wind power samples from the autoregressive model described in Section III, and select a subset of wind time series $a^s \in \mathbb{R}^N, s \in S$, based on a set of prescribed criteria which are deemed important. We then assign weights to each scenario such that the first moments of hourly wind output are matched as closely as possible. That is, we solve the following problem:

$$\min_{\pi_s \in R^S} \sum_{t \in T} \left(\sum_{s \in S} \pi_s a_t^s - \mu_t \right)^2 \qquad (32)$$
$$\text{s.t.}$$
$$\sum_{s \in S} \pi_s = 1 \qquad (33)$$
$$\pi_s \geq 0.01 \qquad (34)$$

where μ_t is the average wind for hour t for the day type that is being considered. The lower bound in (34) is included in order to ensure that all scenarios are considered, albeit with a small weight.

In the results that we present in Section V, we use eleven criteria to select the set of wind time series. The criteria are the following: the series closest to the sampled mean; the series resulting in net load with the greatest variance; the series resulting in net load with the least variance; the series resulting in net load

with the greatest morning up-ramp; the series resulting in net load with the greatest evening up-ramp; the series resulting in net load with the greatest sum of hourly absolute differences; the series resulting in net load with the greatest min-to-max within the day; the series with the least aggregate wind output throughout the day; the series with the greatest aggregate wind output throughout the day; the series resulting in the greatest observed net load peak; and the series resulting in net load with the greatest observed change within one hour. All of these criteria are considered to capture either typical behavior of wind output, or certain anomalous features that need to be explicitly accounted for when scheduling reserves.

V. RESULTS

A. Data

We have used a model of the California ISO with imports from WECC which is developed by the authors in [21]. In contrast to the model that is used in [21], we do not model transmission constraints. We collapse the import schedules of 22 thermal generators outside the California ISO, the export to the Sacramento Municipal Utility District, and the production data from three biomass facilities, six hydroelectric generators, and two geothermal facilities in [21] to a single fixed quantity bid. We do not use the wind production data from [21] since our model contains a much more detailed representation of wind production. Since the model in [21] reflects import, hydroelectric, geothermal, and biomass production data for a six-month period from May 1, 2004, to October 1, 2004, we replicate the data for the remaining six months of the year in order to produce an entire year of data. This extrapolation is justified by the fact that the average production profiles of all these resources are almost identical for the three seasons that are covered by the data-set. Since we are using 2006 wind production data from the NREL database, we also use load data from the same year, which is publicly available at the CAISO Oasis database. The average load in the system is 27 298 MW, with a minimum of 18 412 MW and a peak of 45 562 MW. The net load profile for each type of day, which needs to be served by thermal generators and wind power, is shown in Fig. 1.

The wind data used in this study is sourced from the National Renewable Energy Laboratory 2006 western wind database. The entire data-set is used for calibrating the autoregressive model. The locations of the wind generation sites that are used for the study represent a moderate integration target of 6688 MW, based on the data presented in the CAISO report [1], and a deep integration target of 14 143 MW, corresponding to the 2010 California generation interconnection queue [29]. There is a total of 2648 MW of wind power currently connected in the California system. The locations of the wind parks for each wind integration case are presented in Table II. Wind data was sourced from the NREL database according to the locations that are described in Table II. The wind power production model is described in detail in Section III-C. The penetration level for the moderate integration case is 24.5% of average load capacity and 7.1% of average energy demand, while the penetration level for the deep integration case is 51.8% of average load capacity and 14.0% of average energy demand. In order to identify the

TABLE I
GENERATION MIX FOR THE TEST CASE

Type	No. of units	Capacity (MW)
Nuclear	2	4,499
Gas	86	18,745.6
Coal	6	285.9
Oil	5	252
Dual fuel	23	4,599
Import	22	12,691
Hydro	6	10,842
Biomass	3	558
Geothermal	2	1,193
Wind (7.1% pen.)	5	6,688
Wind (14% pen.)	10	14,143
Fast thermal	82	9,156.1
Slow thermal	40	19,225.4

TABLE II
LOCATIONS AND CAPACITY OF WIND POWER (MW)

County	Existing	7.1% wind	14% wind
Tehachapi	722	4,262	7,181
Clark	-	-	1,500
Solano	327	827	910
San Gorgonio	624	624	1,152
San Diego	-	-	1,527
Humboldt	-	-	218.2
Imperial	-	-	547.9
Altamont	954	954	968
Monterey	-	-	118
Pacheco	21	21	21
Total	2,648	6,688	14,143

two wind integration cases that are analyzed in our study, we label them by their energy penetration level.

We use a finer model for thermal generators within CAISO, with 122 generators, compared to the model in [21], which uses 23 aggregated thermal generators. The value of lost load is set to 5000 $/MWh. The number of generators and the capacity for each fuel type are shown in Table I. The last two rows of Table I describe how the fossil fuel generation mix is partitioned into fast and slow generators. The set of fast generators consists of generators with a capacity no greater than 250 MW, amounting to a total capacity of 9156.1 MW. The entire thermal generation capacity of the system is 28 381.5 MW.

B. Relative Performance of Stochastic Policy

In this section, we compare the performance of the stochastic unit commitment policy with a clairvoyant policy, as well as with common reserve rules. The clairvoyant policy commits reserves with advance knowledge of wind production for each day. The common reserve rules that we consider, peak-load-based unit commitment and the 3+5 rule, are explained in the last paragraph of Section II.

In Fig. 5, we present average cost performance of peak-load-based unit commitment for various levels of total reserve requirements. We see that the optimal reserve requirement for the moderate wind integration level lies at 20% of maximum load, whereas for the deep integration level it lies at 30% of maximum load, and slightly exceeds the policy that commits 40% of maximum load. Reserve requirements that are exceedingly low result in significant load shedding, whereas exceedingly high reserve requirements result in high fuel costs due to the excessive rejection of wind power.
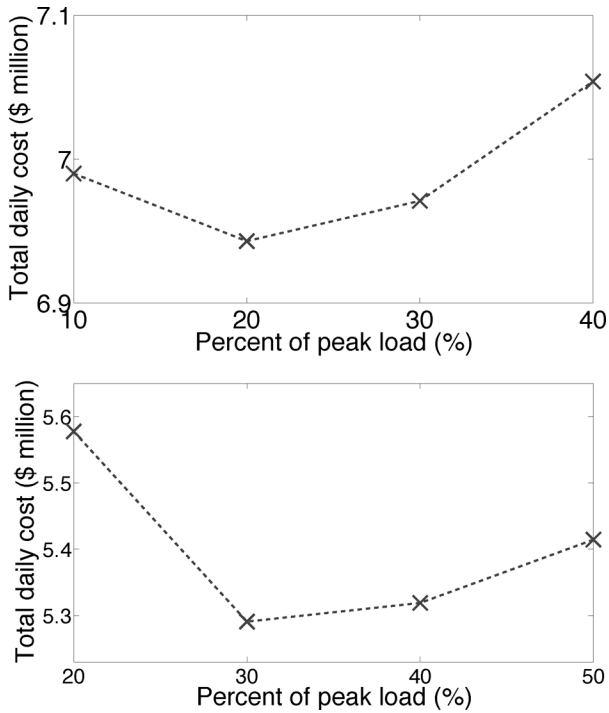
Fig. 5. Cost as a function of total reserve requirements for 7.1% wind (top) and 14% wind (bottom).

TABLE III
DAILY COST OF OPERATIONS FOR EACH DAY TYPE—7.1% WIND

	Cost ($) Stoch	Δ Cost ($) Clair	Δ Cost ($) 20% peak	Δ Cost ($) 3+5
WinterWD	5,970,040	-21,816	20,484	39,747
SpringWD	6,003,520	-37,218	-2,147	14,870
SummerWD	11,272,575	-62,634	102,183	110,793
FallWD	8,081,245	-39,921	15,751	21,618
WinterWE	3,166,890	-32,214	1,346	-3,587
SpringWE	2,642,864	-28,857	-12,622	14,463
SummerWE	7,595,842	-42,179	46,661	46,892
FallWE	5,106,143	-25,350	-1,806	1,002
Total	6,916,442	-38,041	26,733	37,596
improv. (%)		-0.55	0.39	0.54

The lowest possible cost that any unit commitment policy can attain is determined by the performance of a clairvoyant policy, which can anticipate wind generation in advance of unit commitment. In Tables III and IV, we compare the cost performance of the clairvoyant policy, the stochastic policy, the 3+5 rule, and the best peak-load-based policy for the two different wind integration cases. The column with bold figures, which corresponds to the stochastic policy, contains absolute cost values. Cost figures corresponding to the other policies are relative to the stochastic policy costs. The row with total costs weighs the cost of each day type with its relative frequency in the year in order to yield annual results. The last row shows the improvement of the stochastic policy over each other policy, normalized by the cost of the stochastic policy.

The stochastic policy indeed improves on the deterministic policies. The relative savings are greater for the case of deep wind integration. This indicates that the benefits of stochastic unit commitment are larger as uncertainty increases in the system. The clairvoyant policy has a significant advantage over

TABLE IV
DAILY COST OF OPERATIONS FOR EACH DAY TYPE—14% WIND

	Cost ($) Stoch	Δ Cost ($) Clair	Δ Cost ($) 30% peak	Δ Cost ($) 3+5
WinterWD	4,121,453	-169,553	27,642	55,358
SpringWD	3,906,408	-120,016	71,468	103,306
SummerWD	9,773,670	-111,811	147,861	67,553
FallWD	6,125,650	-89,470	27,721	34,900
WinterWE	1,967,672	-75,346	92,732	3,619
SpringWE	1,482,317	-57,696	113,434	96,514
SummerWE	6,309,549	-78,993	79,931	39,757
FallWE	3,524,599	-78,288	-2,508	2,443
Total	5,551,907	-108,389	69,309	56,795
improv. (%)		-2.08	1.33	1.09

TABLE V
SLOW AND TOTAL CAPACITY (MW) FOR EACH POLICY—7.1% WIND

	Stochastic		3+5		20% of peak	
Day Type	Slow	Total	Slow	Total	Slow	Total
WinterWD	8,128	14,811	8,220	17,358	7,946	17,401
SpringWD	8,041	14,910	7,989	17,258	7,858	16,855
SummWD	11,261	20,969	11,646	25,069	11,999	25,254
FallWD	9,173	15,693	9,296	18,531	9,377	18,396
WinterWE	6,044	11,503	6,167	14,702	6,131	13,626
SpringWE	5,804	11,183	6,276	13,991	6,135	14,020
SummWE	9,018	16,647	9,401	21,141	9,443	21,076
FallWE	7,187	12,842	7,028	16,840	6,918	15,907
Total	8,540	15,580	8,696	18,729	8,648	18,528

TABLE VI
SLOW AND TOTAL CAPACITY (MW) FOR EACH POLICY—14% WIND

	Stochastic		3+5		30% of peak	
Day Type	Slow	Total	Slow	Total	Slow	Total
WinterWD	7,012	15,160	7,014	14,856	6,779	14,837
SpringWD	7,818	14,845	6,810	15,889	6,643	15,506
SummWD	10,858	20,766	11,033	24,809	11,555	25,591
FallWD	8,608	16,476	8,417	18,557	8,493	19,143
WinterWE	5,630	11,746	5,569	14,815	5,353	12,010
SpringWE	5,553	11,639	5,670	11,637	5,239	12,151
SummWE	8,759	17,799	8,873	20,956	8,804	21,686
FallWE	6,904	12,823	6,632	15,349	6,687	16,044
Total	8,041	15,866	7,848	17,716	7,840	17,827

the stochastic policy in the deep integration case, versus the moderate case, because greater wind integration exacerbates the level of uncertainty in the system. The 3+5 rule performs better in the deep integration case versus the moderate integration case, compared to the peak-load-based policy. The stochastic policy yields 41% of the potential benefits of having perfect knowledge of the future compared to the best deterministic policy for the 7.1% wind integration case, and 34% of the benefits for the 14% wind case.

We present the total fossil fuel capacity and the average slow generator capacity that is committed for each day type and each policy in Tables V and VI. For the stochastic unit commitment formulation, this table includes the capacity of those slow generators that are committed for at least one hour of the day, or those fast generators that are committed for at least one hour for at least one scenario. For the deterministic unit commitment formulation, this table includes those generators which are required to supply power, slow reserves, or fast reserves for at least one hour of the day. The last line of these tables presents total capacity, which is calculated by weighing the results of each day type by the frequency of occurrence of the respective day type.

TABLE VII
DAILY MWh OF WIND SHED FOR EACH POLICY—7.1% WIND

	Stoch	Clair	3+5	20% peak
WinterWD	5	7	9	10
SpringWD	0	0	0	0
SummerWD	0	0	0	0
FallWD	0	0	0	0
WinterWE	3,034	3,000	3,004	3,033
SpringWE	1,641	1,648	2,145	2,136
SummerWE	0	0	0	0
FallWE	0	0	0.2	0.2
Total	335	333	369	371

TABLE VIII
DAILY MWh OF WIND SHED FOR EACH POLICY—14% WIND

	Stoch	Clair	3+5	30% peak
WinterWD	8,970	7,460	9,446	9,429
SpringWD	8,641	5,438	8,240	8,205
SummerWD	542	453	463	486
FallWD	1,746	1,248	1,697	1,696
WinterWE	28,920	19,721	28,901	28,870
SpringWE	32,261	19,330	32,344	32,040
SummerWE	3,886	3,324	3,731	3,705
FallWE	8,427	5,654	8,376	8,389
Total	8,803	6,038	8,783	8,753

We note that in the 7.1% wind case, the stochastic unit commitment policy tends to commit less total capacity, and less slow capacity. In contrast, in the 14% wind case, the stochastic policy commits more slow capacity and less total capacity. It is interesting to note that the stochastic policy achieves savings with respect to the deterministic policies both in the case where it commits more, as well as less capacity. In the cases where the stochastic policy commits less slow capacity (e.g., summer weekends), the savings result from peak load periods during which the deterministic policies incur large startup costs by committing an excessive amount of slow reserves in order to satisfy reserve requirement constraints. In the cases where the stochastic policy commits more slow capacity (e.g., spring weekdays), the deterministic policies commit less capacity because they underestimate the potential fuel and minimum run savings. This is due to the fact that the deterministic policies optimize for expected wind supply, instead of averaging the cost savings of insuring against fast capacity dispatch for various wind supply outcomes. Due to the fact that fuel and minimum run costs are convex for the system under consideration, deterministic policies underestimate savings from committing slow reserves.

We also present the daily amount of wind that is shed in Tables VII and VIII. In contrast to the results presented in [5], the average wind that is wasted from the clairvoyant policy is less. The losses in the 7.1% wind case are negligible, and the stochastic policy sheds less wind compared to the deterministic policies, which is consistent with the observations in [5]. In the contrary, losses from the stochastic unit commitment policy in the 14% wind case are slightly greater due to the fact that the average slow capacity that is committed in the stochastic policy is greater than the average slow capacity committed in the deterministic policies. Hence we observe that, in order to reduce fuel and startup costs in the 14% wind case, the stochastic policy commits more reserves and sheds slightly more wind power.

TABLE IX
DAILY COST SAVINGS COMPARED TO NO-WIND CASE (%)

Integration	Savings ($)	Min load	Fuel	Load shed	Startup
7.1% wind	1,952,606	8.7	90.4	0.0	0.9
14% wind	3,613,132	7.2	92.4	0.0	0.4

C. Impact of Wind Integration Level

In Table IX, we categorize the cost savings resulting from wind integration. The second column shows the total cost savings for each case of wind integration relative to the case where no wind is integrated. The deep integration case results in almost twice as much savings. The remaining columns refer to the percentage of cost savings that result from each type of cost. Cost savings mainly originate from fuel costs. Load shed costs are insignificant. There are also minor savings from startup costs. For the 14% wind case, the startups required to cope with wind variability tend to reduce the benefits of startup costs.

VI. CONCLUSION

We have developed a two-stage stochastic unit commitment model for determining reserve requirements in the presence of wind power. We have presented a method for generating and weighing the scenarios that are used in the stochastic unit commitment model and we have evaluated our scenario generation methodology by Monte Carlo simulation of unit commitment and economic dispatch. Our stochastic unit commitment schedule is shown to outperform peak-load-based reserve schedules, as well as the 3+5 rule proposed in [22]. Our model is also used to assess the sensitivity of operating costs in wind integration levels. We have omitted various constraints of the unit commitment problem in order to closely analyze our scenario generation methodology. For example, we have not included transmission constraints or import constraints. This is work which we wish to pursue in future research.

APPENDIX

A. Nomenclature for Unit Commitment Problems

Sets

G Set of all generators.

G_s Subset of slow generators.

G_f Subset of fast generators.

S Set of scenarios.

T Set of time periods.

Decision variables

u_{gst} Commitment of generator g in scenario s, period t.

v_{gst} Startup of generator g in scenario s, period t.

p_{gst} Production of generator g in scenario s, period t.

w_{gt} Commitment of slow generator g in period t.

z_{gt} Startup of slow generator g in period t.

s_{gt} Slow reserve provided by generator g in period t.

f_{gt} Fast reserve provided by generator g in period t.

Parameters

π_s — Probability of scenario s.

K_g — Minimum load cost of generator g.

S_g — Startup cost of generator g.

C_g — Marginal cost of generator g.

D_{st} — Net demand[1] in scenario s, period t.

P_g^+, P_g^- — Minimum and maximum capacity of generator g.

R_g^+, R_g^- — Minimum and maximum ramping of generator g.

UT_g — Minimum up time of generator g.

DT_g — Minimum down time of generator g.

N — Number of periods in horizon.

T_{req} — Total reserve requirement.

F_{req} — Fast reserve requirement.

B. Decomposition Algorithm for Stochastic Unit Commtiment

We present a decomposition algorithm for solving the problem presented in (1)–(18). By dualizing the constraints of (15) and (16) we get the following Lagrangian:

$$
\begin{aligned}
\mathcal{L} = &\sum_{g \in G} \sum_{s \in S} \sum_{t \in T} \pi_s (K_g u_{gst} + S_g v_{gst} + C_g p_{gst}) \\
&+ \sum_{g \in G_s} \sum_{s \in S} \sum_{t \in T} \pi_s (\mu_{gst}(u_{gst} - w_{gt}) \\
&+ \nu_{gst}(v_{gst} - z_{gt})).
\end{aligned}
\tag{35}
$$

The first subproblem is, for each scenario

$$
\begin{aligned}
\min &\sum_{g \in G} \sum_{t \in T} \pi_s (K_g u_{gst} + S_g v_{gst} + C_g p_{gst}) \\
&+ \sum_{g \in G_s} \sum_{t \in T} \pi_s (\mu_{gst} u_{gst} + \nu_{gst} v_{gst})
\end{aligned}
\tag{36}
$$

s.t.

$$
(2) - (6), (9), (10), (12), (14)
$$

$$
p_{gst} \geq 0, v_{gst} \geq 0, u_{gst} \in \{0,1\}, g \in G, t \in T. \tag{37}
$$

Note that if we did not impose (12), the previous problem would have been unbounded; therefore, this constraint is necessary for the proposed algorithm. The second subproblem becomes

$$
\min -\sum_{g \in GS} \sum_{s \in S} \sum_{t \in T} \pi_s (\mu_{gst} w_{gt} + \nu_{gst} z_{gt}) \tag{38}
$$

s.t.

$$
(7), (8), (11), (13)
$$

$$
w_{gt} \in \{0,1\}, z_{gt} \geq 0, g \in G_s, t \in T. \tag{39}
$$

The updating of the dual variables is as follows:

$$
\mu_{gst}^{k+1} = \mu_{gst}^k + \alpha_k \pi_s \left(w_{gt}^k - u_{gst}^k \right) \tag{40}
$$

$$
\nu_{gst}^{k+1} = \nu_{gst}^k + \alpha_k \pi_s \left(z_{gt}^k - v_{gst}^k \right). \tag{41}
$$

[1]Net demand refers to demand minus wind.

The step size rule follows [30] and [31] and is given by

$$
\alpha_k = \frac{\lambda \left(\hat{L} - L_k^\star \right)}{\sum_{g,s,t} \pi_s^2 \left(u_{gst}^\star - w_{gt}^* \right)^2 + \pi_s^2 \left(v_{gst}^\star - z_{gt}^\star \right)^2} \tag{42}
$$

where λ is a constant parameter, $L_k^\star$ is the value of (35) at the optimal solution, $\hat{L}$ is an upper bound on the optimal solution, and $u_{gst}^\star, v_{gst}^\star, w_{gt}^\star, z_{gt}^\star$ are optimal solutions at the kth step.

We could have restricted ourselves to relaxing only (15). The advantage of also relaxing (16) is that the first subproblem is smaller, since the constraints on the unit commitment of the slow generators become a part of the second set of subproblems. An additional advantage of this choice of decomposition is that, at each step, the slow generator unit commitment solutions of the first subproblem can be used for generating a feasible solution to the original problem. As a result, at each step of the algorithm, we obtain an upper bound on the optimal solution, as well as a feasible schedule. This should be contrasted to the case where we restrict ourselves to relaxing only (15).

The stochastic unit commitment algorithm was implemented in AMPL. The mixed integer programs were solved with CPLEX 11.0.0 on a DELL Poweredge 1850 server (Intel Xeon 3.4 GHz, 1 GB RAM). The first and second subproblem were run for 200 iterations. For the last 100 iterations, the problem of (1)–(18) was run with $z_{gt}, w_{gt}, g \in G_s, t \in T$ fixed to their optimal values, in order to obtain a feasible solution and an upper bound for the stochastic unit commitment problem of (1)–(18). The average elapsed time for this entire process was 5685 s. The mip gap for the first and second subproblem was set to $\epsilon_1 = 1\%$, and the mip gap for obtaining a feasible schedule was set to $\epsilon_2 = 0.1\%$. The sum of the optimal solutions of the first and second subproblem yield a lower bound LB on the optimal cost, whereas the optimal solution of the feasibility run results in an upper bound UB. The average gap, $(UB - LB)/(LB)$, that we obtained was 0.80%. However, to estimate an upper bound on the optimality gap, we also need to account for the mip gap ϵ_1 that we introduce in the solution of the first and second subproblem. The average upper bound on the optimality gap, $(UB - (1 - \epsilon_1)LB)/((1 - \epsilon_1)LB)$, is 1.75%.

REFERENCES

[1] C. Loutan and D. Hawkins, Integration of Renewable Resources: Transmission and Operating Issues and Recommendations for Integrating Renewable Resources on the California ISO-Controlled Grid, California Independent System Operator, Nov. 2007, Tech. Rep.

[2] R. Gross, P. Heptonstall, D. Anderson, T. Green, M. Leach, and J. Skea, The Cost and Impacts of Intermittency: An Assessment on the Evidence on the Costs and Impacts of Intermittent Generation on the British Electricity Network, UK Energy Research Center, Mar. 2006, Tech. Rep.

[3] R. Zavadil, 2006 Minnesota Wind Integration Study, Enernex Corp., Nov. 30, 2006, vol. I, Tech. Rep.

[4] R. Sioshansi and W. Short, "Evaluating the impacts of real time pricing on the usage of wind power generation," *IEEE Trans. Power Syst.*, vol. 24, no. 2, pp. 516–524, May 2009.

[5] P. A. Ruiz, C. R. Philbrick, and P. W. Sauer, "Wind power day-ahead uncertainty management through stochastic UC policies," in *Proc. Power Systems Conf. Expo.*, Mar. 2009, pp. 1–9.

[6] T. Mount, L. Anderson, J. Cardell, A. Lamadrid, S. Maneevitjit, B. Thomas, and R. Zimmerman, The Economic Implications of Adding Wind Capacity to a Bulk Power Transmission Network Applied Economics and Management, Ithaca, NY, Cornell Univ., 2008, Tech. Rep.

[7] F. Bouffard and F. D. Galiana, "Stochastic security for operations planning with significant wind power generation," *IEEE Trans. Power Syst.*, vol. 23, no. 2, pp. 306–316, May 2008.

[8] J. M. Morales, A. J. Conejo, and J. Perez-Ruiz, "Economic valuation of reserves in power systems with high penetration of wind power," *IEEE Trans. Power Syst.*, vol. 24, no. 2, pp. 900–910, May 2009.

[9] P. A. Ruiz, C. R. Philbrick, E. Zack, K. W. Cheung, and P. W. Sauer, "Uncertainty management in the unit commitment problem," *IEEE Trans. Power Syst.*, vol. 24, no. 2, pp. 642–651, May 2009.

[10] P. A. Ruiz, C. R. Phillbrick, and P. W. Sauer, "Modeling approaches for computational cost reduction in stochastic unit commitment formulations," *IEEE Trans. Power Syst.*, vol. 25, no. 1, pp. 588–589, Feb. 2010.

[11] F. Bouffard, F. D. Galiana, and A. J. Conejo, "Market-clearing with stochastic security: Part I—Formulation," *IEEE Trans. Power Syst.*, vol. 20, no. 4, pp. 1818–1826, Nov. 2005.

[12] S. Takriti, J. R. Birge, and E. Long, "A stochastic model for the unit commitment problem," *IEEE Trans. Power Syst.*, vol. 11, no. 3, pp. 1497–1508, Aug. 1996.

[13] R. T. Rockafellar and R. J.-B. Wets, "Scenarios and policy aggregation in optimization under uncertainty," *Math. Oper. Res.*, vol. 16, no. 1, pp. 119–147, 1991.

[14] P. Carpentier, G. Cohen, J.-C. Culioli, and A. Renaud, "Stochastic optimization of unit commitment: A new decomposition framework," *IEEE Trans. Power Syst.*, vol. 11, no. 2, pp. 1067–1073, May 1996.

[15] T. Shiina and J. R. Birge, "Stochastic unit commitment problem," *Int. Trans. Oper. Res.*, vol. 11, no. 95, pp. 19–32, 2004.

[16] J. Zhang, J. D. Fuller, and S. Elhedhli, "A stochastic programming model for a day-ahead electricity market with real-time reserve shortage pricing," *IEEE Trans. Power Syst.*, vol. 25, no. 2, pp. 703–713, May 2010.

[17] N. Growe-Kuska, K. C. Kiwiel, M. P. Nowak, W. Romisch, and I. Wegner, *Power Management in a Hydro-Thermal System Under Uncertainty by Lagrangian Relaxation*, ser. IMA Volumes in Mathematics and Its Applications. New York: Springer-Verlag, 2002, vol. 128, pp. 39–70.

[18] J. Dupacova, N. Growe-Kuska, and W. Römisch, "Scenario reduction in stochastic programming: An approach using probability metrics," *Math Program.*, no. 95, pp. 493–511, 2003.

[19] H. Heitsch and W. Römisch, "Scenario reduction algorithms in stochastic programming," *Comput. Optimiz. Appl.*, no. 24, pp. 187–206, 2003.

[20] J. M. Morales, S. Pineda, A. J. Conejo, and M. Carrion, "Scenario reduction for futures trading in electricity markets," *IEEE Trans. Power Syst.*, vol. 24, no. 2, pp. 878–888, May 2009.

[21] N.-P. Yu, C.-C. Liu, and J. Price, "Evaluation of market rules using a multi-agent system method," *IEEE Trans. Power Syst.*, vol. 25, no. 1, pp. 470–479, Feb. 2010.

[22] Western Wind and Solar Integration Study, National Renewable Energy Lab., May 2010, Tech. Rep.

[23] R. P. O'Neill, K. W. Hedman, E. A. Krall, A. Papavasiliou, and S. S. Oren, "Economic analysis of the N-1 reliable unit commitment and transmission switching problem using duality concepts," *Energy Syst.*, vol. 1, pp. 165–195, Jan. 2010.

[24] J. L. Torres, A. Garcia, M. D. Blas, and A. D. Francisco, "Time series models to simulate and forecast wind speed and wind power," *J. Climate Appl. Meteorol.*, vol. 23, pp. 1184–1195, Aug. 1984.

[25] J. L. Torres, A. Garcia, M. D. Blas, and A. D. Francisco, "Forecast of hourly wind speed with ARMA models in Navarre (Spain)," *Solar Energy*, vol. 79, no. 1, pp. 65–77, Jul. 2005.

[26] J. M. Morales, R. Minguez, and A. J. Conejo, "A methodology to generate statistically dependent wind speed scenarios," *Appl. Energy*, vol. 87, pp. 843–855, 2010.

[27] D. Callaway, "Sequential reliability forecasting for wind energy: Temperature dependence and probability distributions," *IEEE Trans. Energy Convers.*, vol. 25, no. 2, pp. 577–585, Jun. 2010.

[28] A. C. Harvey, *Time Series Models.*. Cambridge, MA: MIT Press, 1993.

[29] The California ISO controlled grid generation queue as of January 8, 2010. [Online]. Available: http://www.caiso.com/14e9/14e9ddda1ebf0.pdf.

[30] M. L. Fisher, "An applications oriented guide to Lagrangian relaxation," *Interfaces*, vol. 15, no. 2, pp. 10–21, 1985.

[31] W. Held and P. Wolfe, "Validation of subgradient optimization," *Math. Program.*, vol. 6, no. 1, pp. 62–68, Dec. 1974.

Anthony Papavasiliou (S'09) is pursuing the Ph.D. degree in the Department of Industrial Engineering and Operations Research at the University of California at Berkeley. Anthony has interned at the Federal Energy Regulatory Commission, the Palo Alto Research Center and the Energy, Economics and Environment Modelling Laboratory at the National Technical University of Athens. Anthony has received the Sustainable Products and Solutions Program 2010 fellowship.

Shmuel S. Oren (F'02) received the B.Sc. and M.Sc. degrees in mechanical engineering and in materials engineering from the Technion, Haifa, Israel, and the M.S. and Ph.D. degrees in engineering economic systems from Stanford University, Stanford, CA, in 1972.

He is a Professor of IEOR at the University of California at Berkeley and the Berkeley site director of the Power System Engineering Research Center (PSERC). He has published numerous articles on aspects of electricity market design and has been a consultant to various private and government organizations.

Dr. Oren is a Fellow of INFORMS.

Richard P. O'Neill received the B.S. degree in chemical engineering and the Ph.D. degree in operations research from the University of Maryland at College Park.

Currently, he is the Chief Economic Advisor in the Federal Energy Regulatory Commission (FERC), Washington, DC. He was previously on the faculty of the Department of Computer Science, Louisiana State University, Baton Rouge, and the Business School at the University of Maryland at College Park.